

A Dark Matter Model with Non-Abelian Gauge Symmetry

Hao Zhang* and Chong Sheng Li†

*Department of Physics and State Key Laboratory of Nuclear Physics and Technology,
Peking University, Beijing 100871, China*

Qing-Hong Cao‡

*High Energy Physics Divison, Argonne National Laboratory,
Argonne, Illinois 60439, U.S.A. and
Enrico Fermi Institute, University of Chicago, Chicago, Illinois 60637, U.S.A.*

Zhao Li§

*Department of Physics and State Key Laboratory of Nuclear Physics and Technology,
Peking University, Beijing 100871, China and
Department of Physics and Astronomy,
Michigan State University, East Lansing, Michigan 48824, U.S.A*

Abstract

We propose a dark matter model in which the dark sector is gauged under a new $SU(2)$ group. The dark sector consists of $SU(2)$ dark gauge fields, two triplet dark Higgs fields, and two dark fermion doublets (dark matter candidates in this model). The dark sector interacts with the SM sector through kinetic and mass mixing operators. The model explains both PAMELA and Fermi LAT data very well and also satisfies constraints from both the DM relic density and Standard Model precision observables. The phenomenology of the model at the LHC is also explored.

PACS numbers: 95.35.+d, 12.60.-i, 13.90.+i

*Electronic address: haozhang.pku@pku.edu.cn

†Electronic address: csli@pku.edu.cn

‡Electronic address: caoq@hep.anl.gov

§Electronic address: zhaoli@pa.msu.edu

I. INTRODUCTION

Despite that no evidence of new physics signal has been observed at the colliders yet, the observations from cosmology reveal that more than 20% of the whole Universe is made up by the so-called dark matter (DM) [1]. But the Standard Model (SM) does not provide any candidate for the dark matter, so discovering dark matter would be an undoubtable evidence of new physics beyond the SM. Especially, a series of cosmic ray and gamma-ray observations from INTEGRAL [2], ATIC [3], PAMELA [4, 5] and Fermi LAT [6] have attracted extensively attention [7, 8, 9, 10, 11, 12, 13, 14, 15, 16, 17, 18, 19, 20, 21, 22, 23, 24, 25, 26, 27, 28], which indicate that:

- INTEGRAL detected a gamma-ray pick at 511 keV from the center of the galaxy, which can be explained with e^+e^- annihilation there.
- ATIC observed-electron positron excess from 300 GeV to about 800GeV, while the observation from PAMELA shows that there is a positron excess at 10 – 100 GeV.
- Even though the bump-like structure observed by ATIC is not confirmed by Fermi LAT, an excess between 200GeV and 1TeV still remains in the $e^+ + e^-$ spectrum.
- DAMA/LIBRA and DAMA/NaI experiments reported positive results from the direct detection of dark matter [29].

Apparently, it is very exciting to interpret the anomalous signals as being induced by the dark matter. Toward this end, key questions that need to be answered are the following:

- Why is there no hadronic anomaly detected in the cosmic ray experiments?
- Where does the large boost factor ($\sim 10^2 - 10^4$), which is necessary to interpret the positron anomaly as the dark matter signal, originate from?
- What generates the pick near the electron mass pole observed by INTEGRAL?
- Why other direct search experiments do not observe any signal of dark matter?

All those mysterious questions might be related to different aspects of dark matter. Many dark matter models have been proposed to address on one or more questions listed above, but we expect there is a dark matter model which can explain all above experiments very

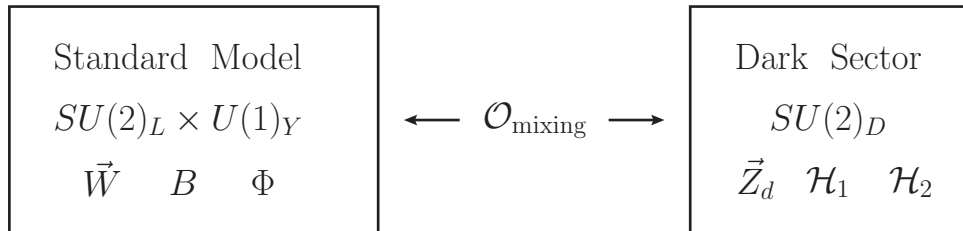


FIG. 1: Sketch of our non-Abelian dark matter model

well. In this work we propose a dark matter model in which the dark sector is gauged under a new $SU(2)$ group. The dark sector consists of $SU(2)$ dark gauge fields, two triplets dark Higgs fields, and two dark fermion doublets (dark matter candidates in this model). The SM sector interacts with the dark sector through kinetic and mass mixing operators. Using two component dark matters, the model could explain both PAMELA and Fermi LAT data very well, while satisfies constraints from both the DM relic density and SM precision observables.

The paper is organized as follows. In Sec. II, we present the field content and the Lagrangian of our model. In Sec. III, we discuss the astrophysics and cosmology observations. In Sec. IV, we show some constraints from the SM precision observables. A global fit to the experimental data is given in Sec. V. In Sec. VI, we analysis the signals of this model at the LHC. Discussions and conclusions are given in Sec. VII. The anomalous dimension and the evolution of the relevant operator, and the decay properties of some new particles are shown in Appendix A and B, respectively.

II. THE DARK MATTER MODEL

In this section, we will propose a specific dark matter model. To answer the questions mentioned above, we adopt some ideas in references [7, 12, 30]. Now we present a non-Abelian dark matter model (NADM) in details. As shown in Fig. 1, our model consists of two sectors: one is the usual SM sector, the other is the dark sector (DS). The SM sector is gauged under the usual $SU(3)_c \times SU(2)_L \times U(1)_Y$ symmetry while the dark sector under a new symmetry $SU(2)_D$ (named as dark symmetry throughout this work). Particles in the dark sector, including the dark matter candidates, neither carry any SM charge nor interact with SM fields directly. Similarly, all the SM particles are invariant under the dark gauge

group transformation. In other words, both sectors are invisible to each other, but they can communicate via (i) the mixing between the SM Higgs boson and dark scalar and (ii) high dimension operators induced by unknown ultraviolet (UV) complete theory at a much higher energy scale Λ . The Lagrangian of our models is

$$\mathcal{L} = \mathcal{L}_{\text{SM}} + \mathcal{L}_{\text{DS}} + \mathcal{L}_{\text{mix}}, \quad (1)$$

where \mathcal{L}_{SM} (\mathcal{L}_{DS}) denotes the Lagrangian of the SM (dark) sector, and \mathcal{L}_{mix} represents the interaction between the SM and dark sectors. Here the dark matter candidates will annihilate into the dark gauge bosons and the dark scalar bosons, which eventually decay into the SM particles via mixing operators.

A. Dark sector

The dark matter candidates in our NADM are Dirac fermion doublets ψ_1 and ψ_2 . The most economic way to obtain anomaly free is to use the vector-like dark fermion. Two or more dark fermion doublets are needed in order to fulfill both XDM [7] and iDM [30] scenarios, because both scenarios require different mass splits between the ground state and excited state of dark matter candidate. For example, the mass split is about 1 MeV in the XDM scenario but about 100 keV in the iDM scenario. In earlier works, some authors suggest the dark matter fermion is dark gauge triplet [12, 31, 32], which does not need two generation DM fermions.

It is worth emphasizing the possibility of multiple dark matter candidates. Many dark-matter candidates have been suggested in various models beyond the SM, but a nearly universal implicit assumption is that only one such candidate is needed and its properties are constrained accordingly. Of course, no fundamental principle requires there is only one dark matter candidate, and the possibility of multipartite dark matter should not be ignored [33, 34, 35, 36, 37, 38]. Moreover, as to be shown later, more than one generation dark matters can fit all experimental data much better in our NADM.

The dark gauge symmetry could be broken in many ways, and one popular choice is with the help of scalar field as the Higgs boson doublet in the SM. However, as pointed out in Ref. [39], the iDM scenario cannot be realized due to a custodial symmetry when only one dark scalar doublet is added. Rather than adding two complex scalar fields, we use two real

scalar triplets (named as dark Higgs boson \mathcal{H}_i) to break the custodial symmetry.

The Lagrangian of the dark sector is

$$\begin{aligned} \mathcal{L}_{\text{DS}} = & -\frac{1}{4}\mathcal{F}_{\mu\nu}^a\mathcal{F}^{\mu\nu a} + \frac{1}{2}\sum_{j=1,2}(D_\mu\mathcal{H}_j^a)(D^\mu\mathcal{H}_j^a) - V_{\mathcal{H}}(\mathcal{H}_1, \mathcal{H}_2) \\ & + \bar{\psi}_1(i\not{D} - m_1)\psi_1 + \bar{\psi}_2(i\not{D} - m_2)\psi_2 + \sum_{j,k=1,2}\beta_{jk}\bar{\psi}_j\mathcal{H}_k\psi_j, \end{aligned} \quad (2)$$

where the dark gauge field tensor $\mathcal{F}_{\mu\nu}^a$, the dark Higgs field covariant derivative D_μ , and the fermion covariant derivative \not{D} are defined by:

$$\mathcal{F}_{\mu\nu}^a = \partial_\mu\mathcal{Z}_\nu^a - \partial_\nu\mathcal{Z}_\mu^a - g_D\epsilon^{abc}\mathcal{Z}_\mu^b\mathcal{Z}_\nu^c \quad (3)$$

$$D_\mu\mathcal{H}_j^a = \partial_\mu\mathcal{H}_j^a - g_D\epsilon^{abc}\mathcal{Z}_\mu^b\mathcal{H}_j^c \quad (4)$$

$$\not{D}\psi_j = \gamma^\mu\left(\partial_\mu\psi_j + ig_D\frac{\sigma^a}{2}\mathcal{Z}_\mu^a\psi_j\right). \quad (5)$$

Here, g_D is dark gauge coupling constant, $V_{\mathcal{H}}$ is the dark scalar potential, β_{jk} is the Yukawa coupling between dark Higgs boson and dark fermions, and m_i is the intrinsic DM fermion mass for ψ_i .

We indicate that after symmetry breaking, both dark gauge bosons \mathcal{Z} and dark fermions ψ_i obtain masses from the dark scalar vacuum condensation, and $m_{\mathcal{Z}}$ is proportional to $g_D v_D$ while m_i to $\beta_{ij} v_D$. As to be discussed below, a large mass hierarchy between \mathcal{Z} and ψ_i , say $m_{\mathcal{Z}} \ll m_i$, is required to fit the PAMELA data. Hence, either a very light \mathcal{Z} or a much heavy ψ_i is preferred. Unfortunately, the former requires a very small dark gauge coupling g_D which will over produce DM relic abundance, and the latter demands a huge Yukawa coupling which will destroy the vacuum stability. In order to avoid these problems, we explicitly keep the intrinsic fermion mass term m_i in \mathcal{L}_{DS} . Such large masses could be generated by other exotic heavy fields which decouple at the scale much higher than the electroweak scale. The Yukawa interaction $\beta_{jk}\bar{\psi}_j\mathcal{H}_k\psi_j$ would generates mass split between the two components inside one fermion doublet.

Last, we comment on the dark scalar potential. When two and more scalar multiplets present, e.g. as in two Higgs doublet model, the scalar potential is rather complicated. Instead of discussing a general scalar potential, we will choose the scalar potential in Eq. 2 as a simple form,

$$V_{\mathcal{H}}(\mathcal{H}_1, \mathcal{H}_2) = \frac{1}{4}\lambda\left(\sum_{j=1,2}(\mathcal{H}_j^a\mathcal{H}_j^a - v_d^2/2)^2 - 2(\mathcal{H}_1^a\mathcal{H}_2^a)^2\right), \quad (6)$$

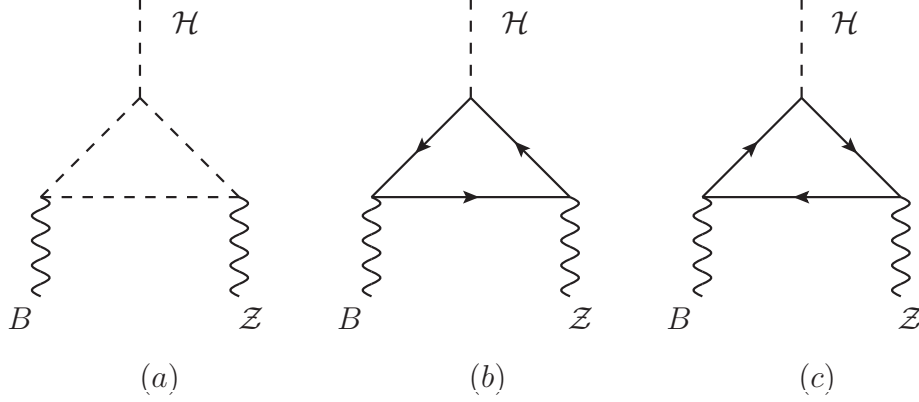


FIG. 2: Representative Feynman diagrams which can induce the dimension-five operator: (a) heavy boson loop, (b) and (c) heavy fermion loop.

which preserves a stable vacuum and breaks the custodial symmetry simultaneously. Here v_d denotes the vacuum expectation value (VEV) of dark Higgs bosons.

B. Interaction between the SM and dark sectors

We first consider that the dark sector interacts with the SM sector through a dimension-5 operator

$$\mathcal{L}_{\text{mix}} \supset -\frac{1}{2\Lambda} B^{\mu\nu} (\alpha_1 \mathcal{H}_1^a + \alpha_2 \mathcal{H}_2^a) \mathcal{Z}_{\mu\nu}^a, \quad (7)$$

where $B^{\mu\nu}$ is the field strength tensor of the gauge boson associated with the SM $U(1)_Y$ group and Λ is the cutoff scale of new physics (NP). Such an operator could be induced by integrating out new heavy particles in a renormalizable theory as shown in Fig. 2, which could generate the dimension-5 operator when new heavy particles decouple. The evolution behavior of this operator is determined by its anomalous dimension (see Appendix A).

Another interaction between the SM and dark sectors is via the mixing between the dark scalar and the SM Higgs boson, such as

$$\mathcal{L}_{\text{mix}} \supset \epsilon_{\mathcal{H}} (\Phi^\dagger \Phi) (\mathcal{H}_1 \cdot \mathcal{H}_2), \quad (8)$$

where Φ denotes the SM Higgs doublet and $\epsilon_{\mathcal{H}}$ is the mixing parameter. Note that the scalar mixing is crucial to prevent overproducing DM relic abundance in our model. For example, without the scalar mixing, there exists a stable dark scalar after symmetry breaking, which could also be dark matter candidate as long as it is lighter than dark fermions. Even

though the dark scalar pair could annihilate into the SM particles through the process $\mathcal{H}\mathcal{H} \rightarrow \gamma\gamma \rightarrow \text{SM particles}$, the annihilation cross section is too small to produce correct amount of relic abundance. In fact, it produces too much relic abundance which would overclose the Universe. Such a problem is solved by the scalar mixing with the SM Higgs boson, which enables the lightest dark scalar decaying into SM fermion.

Next, we discuss some theoretical constraints on $\epsilon_{\mathcal{H}}$:

- *Vacuum stability* : The existence of the lower bound of the scalar potential requires

$$\epsilon_{\mathcal{H}} v_{\text{SM}} v_d / m_H < M_{\mathcal{H}},$$

where v_{SM} and m_H are the vacuum expectation value and the mass of SM Higgs boson (H), respectively.

- *Naturalness* : As pointed out in Ref. [40], the naturalness condition requires that $\epsilon_{\mathcal{H}} v_{\text{SM}}^2$ is not much larger than v_d^2 , i.e.

$$\epsilon_{\mathcal{H}} v_{\text{SM}}^2 \sim v_d^2,$$

which leads to the following bounds: (1) $\epsilon_{\mathcal{H}} \sim 10^{-5}$ for $v_d \sim 1$ GeV and (2) $\epsilon_{\mathcal{H}} \sim 10^{-7}$ for $v_d \sim 0.1$ GeV.

C. Symmetry breaking and mass spectrum of dark particles

In our model the dark $SU(2)_D$ gauge symmetry is broken spontaneously when the two dark scalar triplets develop non-zero vacuum expectation values (VEV). The dark scalar potential achieves its minimum value at

$$\langle \mathcal{H}_1 \rangle = \frac{1}{\sqrt{2}} \begin{pmatrix} 0 \\ 0 \\ v_d \end{pmatrix} \quad \text{and} \quad \langle \mathcal{H}_2 \rangle = \frac{1}{\sqrt{2}} \begin{pmatrix} 0 \\ v_d \\ 0 \end{pmatrix}, \quad (9)$$

where, for simplicity, we choose same VEV (v_d) for both scalar triplets. Therefore, the non-Abelian $SU(2)_D$ symmetry is totally broken by the non-zero v_D .

After dark gauge symmetry breaking, all the three dark gauge bosons become massive:

$$m_{Z_2} = m_{Z_3} = M_Z = g_D v_d, \quad \text{and} \quad m_{Z_1} = \sqrt{2} M_Z. \quad (10)$$

The dark gauge boson mass will be modified slightly when they mix with SM gauge bosons through the operator as shown in Eq. 7. Without losing generalization, we choose $\alpha_1 = 0$ in Eq. 7. As a result, only \mathcal{Z}_2 mixes with SM gauge boson. Note that a non-zero α_1 merely changes the definition of mass eigenstates, and there is still only one dark gauge boson mixing with SM gauge boson directly. Then, the kinematic mixing between $U(1)_Y$ gauge boson and \mathcal{Z}_2 generated by this operator is

$$\mathcal{L}_{KM} = -\frac{\epsilon}{2} B_{\mu\nu} \mathcal{Z}_2^{\mu\nu}, \quad (11)$$

where $\epsilon = \alpha_2 v_d / \sqrt{2} \Lambda$, and $\mathcal{Z}_2^{\mu\nu} = \partial^\mu \mathcal{Z}_2^\nu - \partial^\nu \mathcal{Z}_2^\mu$. It leads to non-diagonal elements in the kinetic energy term of Lagrangian in the basis $\hat{V}_\mu^T = (\hat{\mathcal{Z}}_{2\mu}, \hat{B}_\mu, \hat{W}_{3\mu})$

$$\mathcal{K} = \begin{pmatrix} 1 & \epsilon & 0 \\ \epsilon & 1 & 0 \\ 0 & 0 & 1 \end{pmatrix}, \quad (12)$$

where the gauge field with a caret symbol is understood as the current eigenstate. Furthermore, the mass matrix takes the following form

$$\mathcal{M}^2 = \begin{pmatrix} M_{\mathcal{Z}}^2 & 0 & 0 \\ 0 & \frac{1}{4} v_{SM}^2 g_Y^2 & -\frac{1}{4} g_2 g_Y \\ 0 & -\frac{1}{4} v_{SM}^2 g_2 g_Y & \frac{1}{4} v_{SM}^2 g_2^2 \end{pmatrix} \quad (13)$$

We denote the mass eigenstates of the three gauge bosons by $V_\mu^T = (\mathcal{Z}_{2\mu}, A_\mu, Z_\mu)$. A simultaneous diagonalization of both the kinetic energy term and the mass matrix gives (to order ϵ)

$$\begin{aligned} \hat{B}^\mu &= A^\mu c_W - Z^\mu s_W + \left(\frac{\tilde{m}_Z^2 s_W^2}{\tilde{m}_Z^2 - M_{\mathcal{Z}}^2} - 1 \right) \epsilon \mathcal{Z}_2^\mu, \\ \hat{W}_3^\mu &= A^\mu s_W + Z^\mu c_W - \frac{\tilde{m}_Z^2 s_W c_W \epsilon}{\tilde{m}_Z^2 - M_{\mathcal{Z}}^2} \mathcal{Z}_2^\mu, \\ \hat{\mathcal{Z}}_2^\mu &= \mathcal{Z}_2^\mu + \frac{\tilde{m}_Z^2 s_W \epsilon}{\tilde{m}_Z^2 - M_{\mathcal{Z}}^2} Z^\mu, \end{aligned} \quad (14)$$

where $s_W \equiv \sin \theta_W = g_Y / \sqrt{g_2^2 + g_Y^2}$, $c_W \equiv \cos \theta_W = g_2 / \sqrt{g_2^2 + g_Y^2}$. And the masses of the corresponding mass eigenstates are given by (to order of ϵ^2)

$$\begin{aligned} m_A^2 &= 0, \\ m_Z^2 &= \tilde{m}_Z^2 \left(1 + \frac{\tilde{m}_Z^2 s_W^2}{\tilde{m}_Z^2 - M_{\mathcal{Z}}^2} \epsilon^2 \right), \\ m_{\mathcal{Z}_2}^2 &= M_{\mathcal{Z}}^2 \left(1 - \frac{\tilde{m}_Z^2 s_W^2}{\tilde{m}_Z^2 - M_{\mathcal{Z}}^2} \epsilon^2 \right), \end{aligned} \quad (15)$$

where $\tilde{m}_Z (= g_2 v_{SM} / 2c_W)$ is the SM Z -boson mass. The gauge fields in the mass eigenstate basis are (to order of ϵ)

$$\begin{aligned} A^\mu &= c_W \hat{B}^\mu + s_W \hat{W}_3^\mu - \epsilon \hat{Z}_2^\mu c_W, \\ Z^\mu &= c_W \hat{W}_3^\mu - s_W \hat{B}^\mu + \epsilon \frac{M_Z^2 s_W}{\tilde{m}_Z^2 - M_Z^2} \hat{Z}_2^\mu, \\ \mathcal{Z}_2^\mu &= \hat{Z}_2^\mu + \epsilon \frac{\tilde{m}_Z^2 s_W}{\tilde{m}_Z^2 - M_Z^2} (c_W \hat{W}_3^\mu - s_W \hat{B}^\mu). \end{aligned} \quad (16)$$

Two dark scalar triplets carry six degrees of freedom. While three of them are eaten by dark gauge boson after symmetry breaking, the rest three remain as three physical dark scalar fields. In the unitary gauge, the two scalar triplets can be written as

$$\mathcal{H}_1 = \begin{pmatrix} 0 \\ h_3/\sqrt{2} \\ h_1 + v_d/\sqrt{2} \end{pmatrix} \quad \text{and} \quad \mathcal{H}_2 = \begin{pmatrix} 0 \\ h_2 + v_d/\sqrt{2} \\ h_3/\sqrt{2} \end{pmatrix}, \quad (17)$$

where h_1 , h_2 and h_3 are physical dark scalars with degenerate mass $M_{\mathcal{H}}^2 = \lambda_D v_d^2 = \lambda_D M_Z^2 / g_D^2$. In addition the mixing term in Eq. 8 can induce the following mass matrix in the basis (H_0, h_3)

$$\frac{1}{2} \begin{pmatrix} H_0 & h_3 \end{pmatrix} \begin{pmatrix} m_H^2 & \epsilon_{\mathcal{H}} v_d v_{SM} \\ \epsilon_{\mathcal{H}} v_d v_{SM} & M_{\mathcal{H}}^2 \end{pmatrix} \begin{pmatrix} H_0 \\ h_3 \end{pmatrix}. \quad (18)$$

Thus, the mass eigenstates and their masses are given by

$$\begin{aligned} \tilde{h}_3 &= h_3 - \frac{\epsilon_{\mathcal{H}} v_d v_{SM}}{m_H^2 - M_{\mathcal{H}}^2} H_0, \quad m_{\tilde{h}_3}^2 = M_{\mathcal{H}}^2 - \frac{\epsilon_{\mathcal{H}}^2 v_d^2 v_{SM}^2}{m_H^2 - M_{\mathcal{H}}^2} \\ \tilde{H}_0 &= H_0 + \frac{\epsilon_{\mathcal{H}} v_d v_{SM}}{m_H^2 - M_{\mathcal{H}}^2} h_3, \quad m_{\tilde{H}_0}^2 = m_H^2 + \frac{\epsilon_{\mathcal{H}}^2 v_d^2 v_{SM}^2}{m_H^2 - M_{\mathcal{H}}^2}. \end{aligned} \quad (19)$$

The dark Higgs boson \tilde{h}_3 is no longer stable as it can decay to SM fermion pair through the above mixing.

III. ASTROPHYSICS AND COSMOLOGY OBSERVATIONS

A. Dark matter relic density

In our model the dominant contribution to dark matter annihilation comes from the channels involving dark gauge boson and dark Higgs (also with the lighter generation dark

fermion for the heavier generation freezing out) in the final state, which is of order α_D^2 . Those annihilation products decay into the SM particles eventually. Below we calculate the relic abundance in our model following Ref. [41]. Furthermore, coannihilation effects [42] are also considered in our calculation, as the masses of the two component fields of DM fermion doublet are nearly degenerated.

As to be shown later, in order to fit both PAMELA and Fermi LAT data in our model, it is necessary to have a large mass splitting between ψ_1 and ψ_2 . Therefore, the DM annihilation involves the dark gauge interaction at different energy scales. Running effect of dark gauge coupling has to be considered in the numerical evaluation. The running behavior of dark gauge coupling is governed by renormalization group equation (RGE). The one-loop level beta function for a general non-Abelian gauge theory is [43]

$$\beta(g) = \frac{g^3}{16\pi^2} \left(-\frac{11}{3}N + \frac{1}{6}C_{2b} + \frac{4}{3}C_{2f} \right). \quad (20)$$

In our model, $N = 2$, $C_{2b} = 2n_b$ and $C_{2f} = \frac{n_f}{2}$, where $n_b = 2$ is the number of real Higgs triplet, n_f is the number of fermion doublet. For the energy scale $\mu > m_2$, $n_f = 2$, for $m_1 < \mu < m_2$, $n_f = 1$, and for $\mu < m_1$, $n_f = 0$. Within this theoretical framework, the dark gauge interaction is asymptotic free, i.e. becoming stronger at low energy but weaker at high energy. In this work we choose the following parameters as benchmark:

$$\begin{aligned} m_1 &= 510 \text{ GeV} , \quad m_2 = 1300 \text{ GeV}, \\ M_{\mathcal{Z}} &= 0.1 \text{ GeV} , \quad M_{\mathcal{H}} = 0.02 \text{ GeV}, \end{aligned} \quad (21)$$

to explore the impact of RG running effect on the relic abundance.

Figure 3(a) displays the relic density versus dark gauge boson coupling at the scale $\mu = M_{\mathcal{Z}}$. Note that, with running effects, the dark gauge coupling is evaluated at the scale $\mu = 2m_i$ in the numerical calculation of DM annihilation cross sections. It is well known that the relic density of DM is approximately given by $\Omega h^2 \approx (0.1 \text{ pb}) / \langle \sigma v \rangle$ where $\langle \sigma v \rangle$ is the thermally averaged product of the DM annihilation cross section with its velocity. Five-year WMAP data indicates $\langle \sigma v \rangle \simeq \text{pb}$. Since the final state particles in the DM annihilation are almost massless, the annihilation cross section can be written as following, based on the dimension counting,

$$\sigma_i v \propto \frac{g_D^2}{m_i^2}. \quad (22)$$

When the DM candidate masses are given, there exists an unique dark gauge coupling to produce the correct amount of relic abundance. For example, without running effect, the correct relic density can be produced only in the vicinity of $\alpha_D \sim 0.1$; see the black curve in Fig. 3(a). With running effects, the gauge coupling at the scale $\mu = 2m_i$ is less than its value at the scale $\mu = M_Z$, therefore, large coupling strength is needed to induce efficient DM annihilation; see the red curve in Fig. 3(a). Owing to the RG running effect, the favored coupling region, which is consistent with the WMAP data at 1σ level (green band), become much broader (e.g. $0.45 < \alpha_D < 0.67$) for the given benchmark parameters.

In Fig. 3(b), we display the comparison of two dark matters (red) and one dark matter (black). In the case of one generation dark matter, we fix its mass be 1300 GeV because the Fermi LAT data prefers a very heavy DM candidate. It is clear that the model cannot produce a correct DM relic density when only one heavy DM candidate presents, even for an unreasonably large coupling such as $\alpha_D \sim 5$. It is due to the heavy mass suppression in Eq. 22 which yields a small DM annihilation rate, cf. the black curve. Introducing another generation dark matter efficiently reduces relic density to satisfy the WMAP data, cf. the red curve.

B. INTEGRAL and XDM

As pointed out in Ref. [7], if dark matter has an excited state and the mass split is about $2m_e$, decay of the excited state of dark matter may produce much e^+e^- as a source of the gamma-ray line in the galactic center at 510.954 ± 0.075 keV confirmed by INTEGRAL/SPI [44]. Following the proposal in Ref. [7], we find that in our model the dark gauge boson mass M_Z should be less than 0.2 GeV in order to give a significant contribution to the 511 keV signal. As a result, such a light dark gauge boson cannot decay into quarks, muon and tau due to the kinematics.

C. PAMELA and Fermi LAT

To fit the data of PAMELA and Fermi LAT, we calculate the cosmic ray e^+e^- flux, using the background flux formula [45] and the formulas of the dark-matter-induced flux [46]. In Appendix B we summarize the decay properties of dark gauge boson and dark scalars used

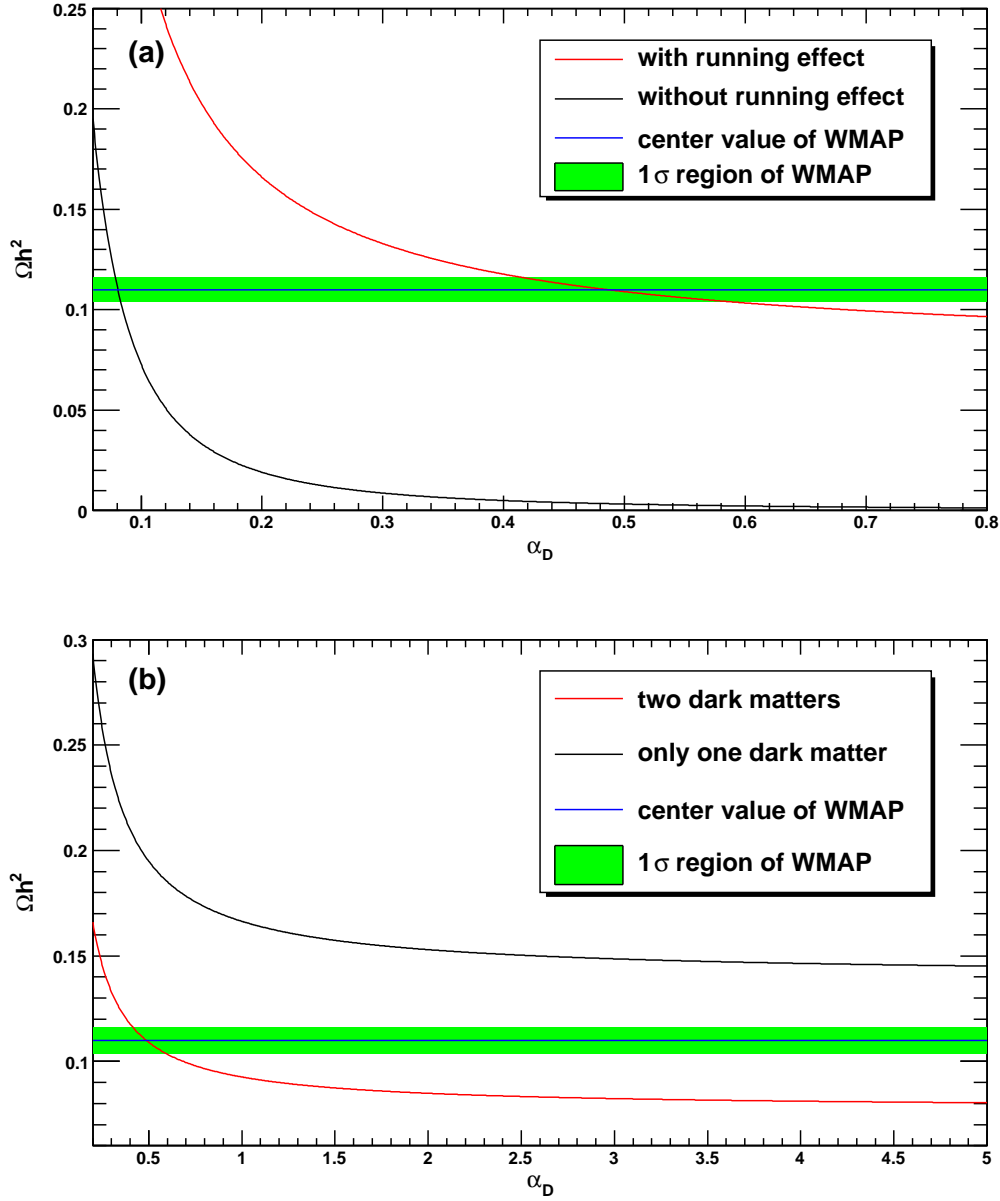


FIG. 3: (a) Relic abundance versus dark gauge coupling evaluated at the scale M_Z , with and without running effect of dark gauge boson. The annihilation cross sections are calculated with the dark gauge coupling at the scale $\mu = 2m_i$. The parameters are chosen to be $m_1 = 510$ GeV, $m_2 = 1300$ GeV, $M_Z = 0.1$ GeV and $M_{\mathcal{H}} = 0.02$ GeV. The dark green band display the cold dark matter density from Five-Year WMAP data, $\Omega h^2 = 0.1099 \pm 0.0062$ [1]. (b) Comparison of two generation DMs and one generation DM with the choice of above parameters, except that we fix the DM mass be 1300 GeV in the one dark matter case.

in our numerical calculation. The large Sommerfeld enhancement factor, which is given by the non-Abelian dark gauge interaction, can be calculated numerically following Ref. [47]. The results of fitting PAMELA and Fermi LAT is shown below.

D. Direct detection of dark matter

Current direct detection experiments of dark matter [29, 48, 49, 50] give negative result except DAMA [29]. In our model, the interaction between dark matters and nucleon is iDM like [30], so the direct detection can not give a strong limit to ϵ . For the generation whose mass split is greater than $2m_e$ required by XDM, the corresponding critical velocity [30] will be larger than the escape velocity of dark matter in the galaxy, which means that it can not be detected in the direct detection experiments. For another generation, the mass split is still a free parameter which can be use to explain DAMA and other direct detection experiments data.

IV. CONSTRAINTS FROM THE SM PRECISION OBSERVABLES

Due to its mixing with the SM gauge bosons, the dark gauge boson inevitably modifies various low energy precision observables, such as the oblique parameters [51], muon anomalous magnetic momentum, and Z^0 boson decay, etc. In this section we explore constraints from those precision measurements.

a. The Electroweak Oblique Parameters The oblique parameters S , T and U can be calculated with formulas in Ref. [52]. In our model, to the order of ϵ^2 ,

$$\begin{aligned} S &= \frac{2\sqrt{2}\pi\epsilon^2}{G_F(m_Z^2 - M_Z^2)}, \\ T &= \frac{\pi\epsilon^2}{\sqrt{2}c_W G_F(m_Z^2 - M_Z^2)}, \\ U &= 0, \end{aligned} \tag{23}$$

where G_F is the Fermi constant. For $M_Z \sim 0.1$ GeV, from above parameters we can get $\epsilon \lesssim 0.023$ at 1σ level.

b. Muon Anomalous Magnetic Moment The additional contribution to the muon anomalous magnetic moment $(g-2)_\mu$ is mainly from \mathcal{Z}_2 , which can be calculated by [53]

$$F_2(0) = \frac{2g_2^2}{m_{\mathcal{Z}_2}^2} m_\mu^2 \int_0^1 dz(1-z) \int \frac{d^4k}{(2\pi)^4} \frac{1}{(k^2+b^2)^3} \left(h_1(z) + \frac{g_1^2}{g_2^2} h_2(z) \right), \quad (24)$$

with

$$h_1(z) = -4z(z+3), \quad (25)$$

$$h_2(z) = 4z(1-z), \quad (26)$$

$$b^2 = z + \frac{m_\mu^2}{m_{\mathcal{Z}_2}^2} (1-z)^2, \quad (27)$$

and

$$\begin{aligned} g_1^2 &= \frac{e^2 \epsilon^2}{16c_W^2} \left[4c_W^2 + \frac{M_{\mathcal{Z}}^2}{M_Z^2} (1 - 4s_W^2) \right]^2, \\ g_2^2 &= \frac{e^2 \epsilon^2}{16c_W^2} \frac{M_{\mathcal{Z}}^4}{M_Z^4}, \end{aligned} \quad (28)$$

where m_μ is the muon mass. For $\epsilon \lesssim 7 \times 10^{-4}$, the contribution from \mathcal{Z}_2 to $(g-2)_\mu$ is less than 10^{-10} . Here we choose $M_{\mathcal{Z}} \sim 0.1\text{GeV}$ and $M_{\mathcal{H}} \sim 0.02\text{GeV}$.

The contribution from \tilde{h}_3 is much less than \mathcal{Z}_2 . Even for $\epsilon_{\mathcal{H}} \sim 400$ the contribution from \tilde{h}_3 to $(g-2)_\mu$ is less than 10^{-10} when $M_{\mathcal{Z}} \sim 0.1\text{GeV}$ and $M_{\mathcal{H}} \sim 0.02\text{GeV}$. These results show that the constraint from $(g-2)_\mu$ is not strong.

c. Decay width of the SM Z^0 Boson In our model there are some new decay channels of the SM Z^0 : $Z^0 \rightarrow \mathcal{Z}_1 \mathcal{Z}_3$, $Z^0 \rightarrow \mathcal{Z}_2 h_1$, $Z^0 \rightarrow \mathcal{Z}_2 h_2$, $Z^0 \rightarrow \mathcal{Z}_2 \tilde{h}_3$, $Z^0 \rightarrow \mathcal{Z}_3 \tilde{h}_3$, $Z^0 \rightarrow \gamma h_2$. Ignoring the higher order terms of $M_{\mathcal{H}}^2/m_Z^2$ and $M_{\mathcal{Z}}^2/m_Z^2$, to the order of ϵ^2 , the non-zero decay widths are

$$\Gamma_{\mathcal{Z}_1 \mathcal{Z}_3}^Z = \Gamma_{\mathcal{Z}_2 h_2}^Z = 2\Gamma_{\mathcal{Z}_3 \tilde{h}_3}^Z = \frac{\alpha_D \epsilon^2 s_W^2 m_Z^3}{12M_{\mathcal{Z}}^2}, \quad (29)$$

$$\Gamma_{\mathcal{Z}_2 h_1}^Z = \frac{\alpha_D \epsilon^2 s_W^2 m_Z}{24}. \quad (30)$$

From above results and the experimental data of the Z^0 decay width [54], at 1σ level, ϵ should be less than 4.5×10^{-5} for $M_{\mathcal{Z}} \sim 0.1\text{GeV}$, $\alpha_D(M_{\mathcal{Z}}) = 0.57$ and $M_{\mathcal{H}} \sim 0.02\text{GeV}$. Our calculation shows that the evolution of the operator in Eq. 7 is negligible small (see Appendix A).

V. EXPLANATION OF THE PAMELA AND FERMI LAT OBSERVATIONS

In this section, we present a global fit of the PAMELA, Fermi LAT, DM relic density, the S and T parameters, and Z^0 boson decay width, using least χ^2 analysis [55, 56]. As widely used in the literatures, a parameter b_k is introduced to rescale the cosmic ray background here. In general, the total distribution of dark matter in the galaxy can be determined by N-body simulations, but for a model of two generation dark matters, the fraction of each generation in the galaxy is unknown. In our model, since the masses of two dark matters are different, the ratio r_{galaxy} of their total masses in the galaxy will be different from $r_{\text{freeze}} = \Omega_{\text{heavy}}/\Omega_{\text{light}}$, where $\Omega_{\text{heavy}}(\Omega_{\text{light}})$ is the relic density of the heavier (lighter) dark matter. So we take r_{galaxy} as a free parameter.

In our fitting we require the theoretical values of both the SM relevant precision observables and the relic density fall in 1σ region of the experimental data. We fit the PAMELA and Fermi LAT data using NFW profile [57] and “MED” propagation scheme [46]. The best-fit solution is $\alpha_D(M_Z) = 0.57$, $M_Z = 0.1$ GeV, $M_{\mathcal{H}} = 0.02$ GeV, $m_1 = 510$ GeV, $m_2 = 1300$ GeV, $\epsilon = 10^{-5}$, $b_k = 0.66$ and $r_{\text{galaxy}} = 6.1$, resulting in $\chi^2 = 1.1$ per degree of freedom.

We illustrate, in Fig. 4(a), the positron fraction as seen at Earth after propagating effects are included in the “MED” propagation scheme [46]. We note that our best fit is quite good, with the Sommerfeld enhancement boost factor of $\sim 5 \times 10^3$ in our case. The kink at the high energy region is due to the overlap of cosmic positrons from two component DM annihilations. Figure 4(b) shows that our model prediction also fits the Fermi LAT very well. With enough precision, the kink feature of two component dark matters may be explored in future experiments.

VI. LHC PHENOMENOLOGY

The typical signals of our model at the LHC are the lepton jets, which are boosted groups of $n \geq 2$ leptons with small angle separations and GeV scale invariant masses as shown in Ref. [66]. Especially, for the process $p + p \rightarrow Z^0 \rightarrow \mathcal{Z}_2 + h_2 \rightarrow e^+e^- + \cancel{E}_T$, the signal is just one lepton jet originated from the \mathcal{Z}_2 decay plus \cancel{E}_T from the long lived h_2 . See Appendix B for detailed calculation of the dark gauge boson and dark scalar decays. The intrinsic SM

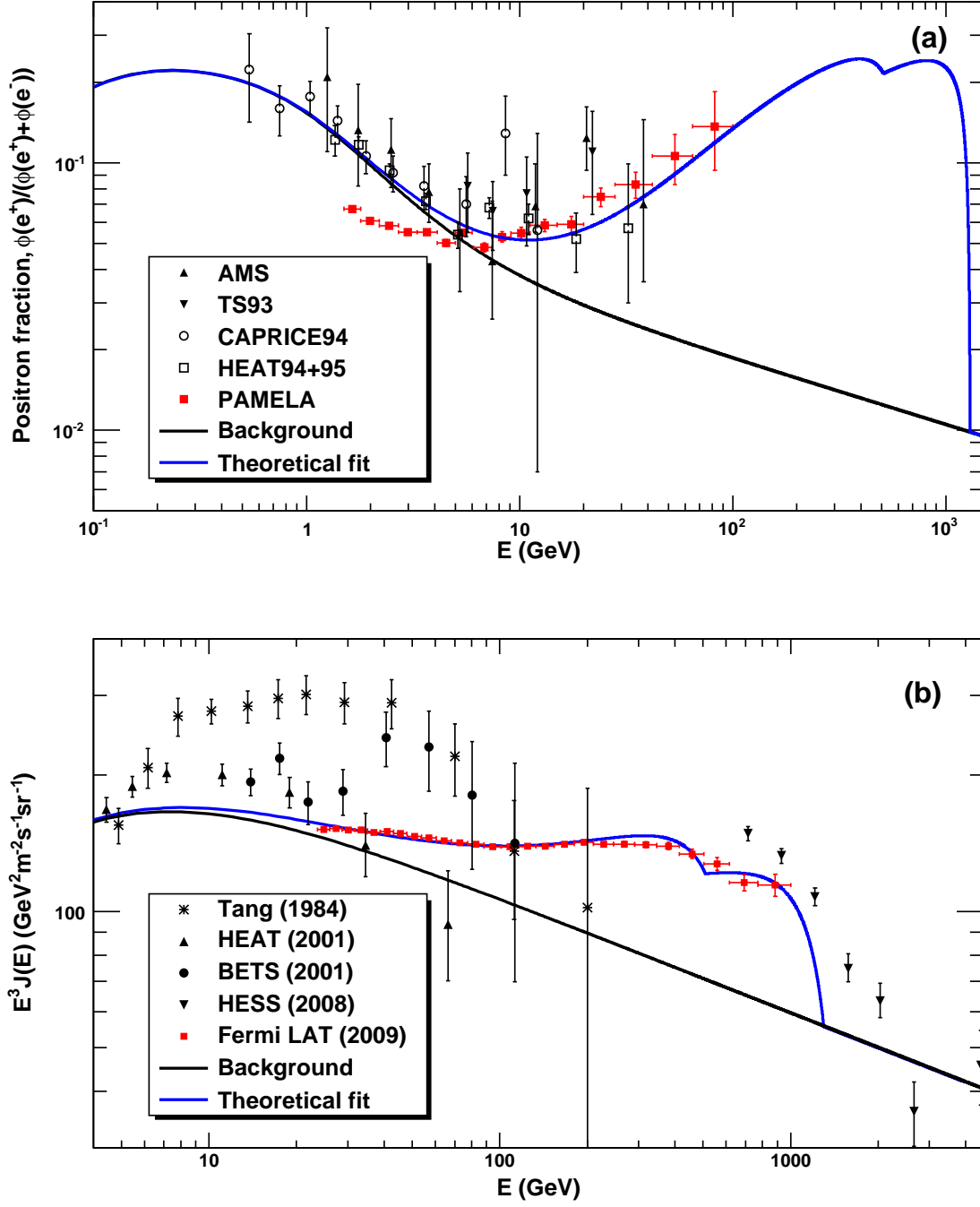


FIG. 4: (a) Fit to PAMELA data of this model at the minimum χ^2 parameter point where the experiments data can be found in [4, 58, 59, 60, 61]; (b) Fit to Fermi LAT data of this model at the minimum χ^2 parameter point where the experiments data can be found in [6, 62, 63, 64, 65].

backgrounds originate from the W^+W^- and $ZZ/Z\gamma^*$ pair production. Only the $W \rightarrow e\nu_e$ decay mode is considered in the WW background in order to mimic the signal signature. Similarly one of the Z boson has to decay into neutrino pair and the other Z boson or off-shell photon decays into electron-positron pair. With the help of CalcHEP [67], we examine the kinematics distributions of both signal and background.

Kinematics of the signal process is very distinctive from those of background processes:

- *Signal:* The two charged leptons in the signal are forced to move collaterally due to the large boost received from \mathcal{Z}_2 . Even though it is challenging to measure the momentum of each charged lepton, one can measure the sum of the energy and transverse momentum (p_T) of the two charged lepton system. The distribution of $p_T^{e^+e^-}$ as well as \cancel{E}_T peaks around half of the Z^0 boson mass; see the red-dotted curve in Fig. 5. Similar to the $W \rightarrow \ell\nu$ decay, the transverse mass of the lepton-jet and missing transverse momentum \cancel{E}_T also exhibit a sharp Jacobin peak around m_{Z^0} . On the other hand, the invariant mass of the leptons is around GeV. Last, the \mathcal{Z}_2 boson is long lived with $\epsilon = 10^{-5}$. It, when produced, will propagate about 30 centimeter inside the detector, which provides an unique collider signature.
- *WW background:* The two charged leptons in the WW background neither move parallel to each other nor exhibit GeV invariant mass peak.
- *ZZ background:* Since the dominant contribution is from the on-shell Z boson production, the invariant mass of two charged leptons is close to m_{Z^0} . The distribution of $p_T^{e^+e^-}$, i.e. $p_T^{Z^0}$, peaks around 30 GeV.
- *$Z\gamma^*$ background:* It provides very similar collider signature as the signal. Originated from a off-shell photon decay, two charged leptons move in parallel and have a small invariant mass. The transverse mass of the lepton system and \cancel{E}_T does not peak around m_{Z^0} . Unlike the signal, the off-shell photon decays promptly and do not travel a long distance inside the detector.

The SM backgrounds, mainly from WW production, overwhelm the signal. Making use of the kinematics difference mentioned above, one can impose optimal cuts to suppress the SM background. For illustration, we impose the following two simple cuts:

$$m_{e^+e^-} < 10 \text{ GeV} \quad \text{and} \quad \cos\theta_{e^+e^-} > 0.95, \quad (31)$$

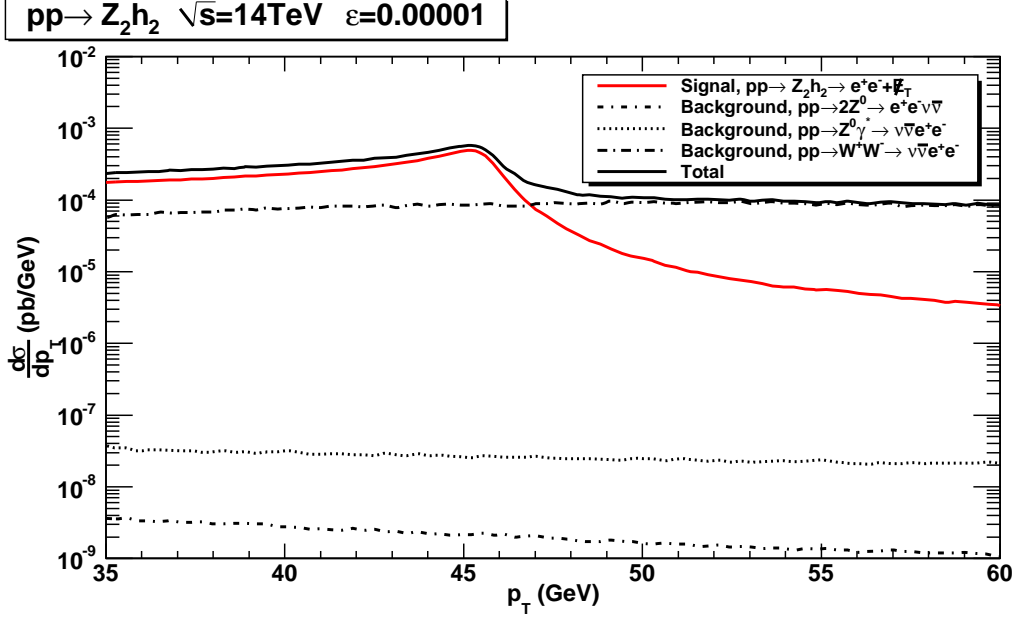


FIG. 5: Differential distribution of transverse momentum of the lepton jet system $p_T^{e^+e^-}$ with the cuts: $m_{e^+e^-} < 10\text{GeV}$ and $\cos\theta_{e^+e^-} > 0.95$.

where $m_{e^+e^-}$ is the invariant mass of lepton-jets and $\theta_{e^+e^-}$ is the open polar angle between the electron and positron. Figure 5 shows the $p_T^{e^+e^-}$ distributions of signal and background with the cuts in Eq. 31, which clearly shows that it is very promising to observe the dark gauge boson signal at the LHC. However, one should bear in mind that the above two cuts serve for the purpose of suppressing the SM background processes. It is crucial to understand how well one can measure the energy and momentum of the lepton jets, which is beyond the scope of this paper and will be presented in the future work.

VII. CONCLUSIONS

Discovering dark matter would be an undoubted evidence of new physics beyond the Standard Model. Recently, many excesses were observed in the direct and indirect search of dark matter [2, 3, 4, 5, 6, 29]. In this work we proposed a non-Abelian dark matter model to explain all those observed excesses. The model consists of both SM sector and dark sector. The latter, gauged under a new $SU(2)$ dark gauge symmetry, contains $SU(2)$ dark gauge boson fields, two triplets dark Higgs fields and two generation dark fermion doublets (dark matter candidates). Rather than considering only one dark matter candidate, we introduced

two coexisting stable dark matters: one is around 500 GeV and the other is around 1300 GeV. Our study shows that two dark matter scenario naturally fits both PAMELA and Fermi LAT data simultaneously. Dark matter annihilation occurs in the dark sector and the remanent dark particles (dark gauge boson and dark scalars) decay into the SM particles eventually through the kinetic and mass mixing operators between the SM and dark sectors. The triplet dark scalars are introduced to break the dark gauge symmetry and also generate small mass splits between the two component fields of dark fermion doublets. Such small mass splits is the key to realize the iDM and XDM scenarios, which explain the INTEGRAL and DAMA results. Finally, we explore the interesting collider signature of the dark gauge boson and dark scalar production at the LHC. Our simulation analysis indicates that the signals of this model may be detectable at the LHC.

In our model, since the Lagrangian of the dark sector has scalar mass terms, there is a dark sector fine tuning problem. In general, such a fine tuning problem can be solved by introducing supersymmetry in the dark sector. The supersymmetry extension of this model will be especially interesting and will be presented elsewhere.

Acknowledgments

This work is supported in part by the National Natural Science Foundation of China, under Grants No.10721063, No.10975004 and No.10635030. Q. H. C. is supported in part by the Argonne National Laboratory and University of Chicago Joint Theory Institute (JTI) Grant 03921-07-137, and by the U.S. Department of Energy under Grants No. DE-AC02-06CH11357 and No. DE-FG02-90ER40560. Zhao Li is supported in part by the U.S. National Science Foundation under Grant No. PHY-0855561.

APPENDIX A: ANOMALOUS DIMENSION OF THE OPERATOR

In this appendix, we show the evolution of the dimension-five operator in Eq. 7, since the operator evolution can change the theoretical result significantly [68]. The evolution of the Wilson coefficient $C(\mu)$ of the effective Hamiltonian $\frac{1}{2\Lambda}C(\mu)\mathcal{O}(\mu)$ ($\mathcal{O} \equiv B_{\mu\nu}\mathcal{Z}^{a,\mu\nu}\mathcal{H}_2^a$) is determined by the evolution equation

$$\mu\frac{d}{d\mu}C = \gamma_{\mathcal{O}}C, \quad (\text{A1})$$

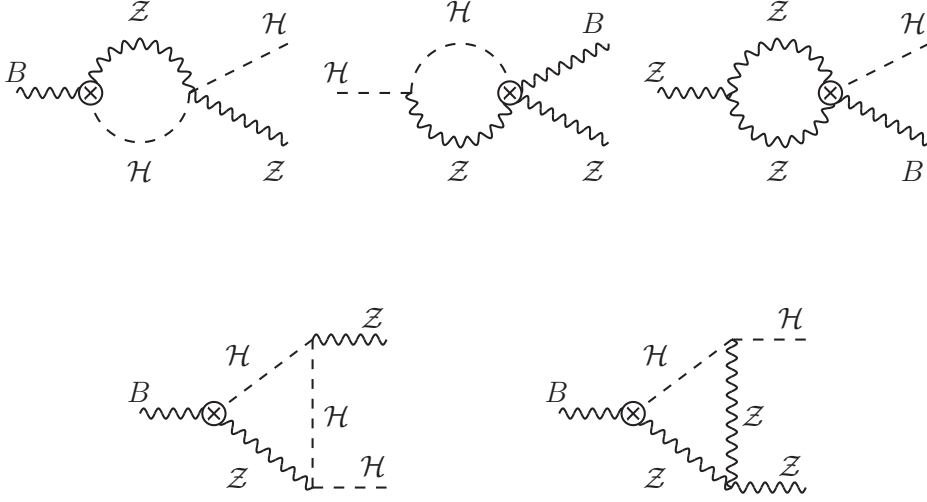


FIG. 6: The feynman diagrams which contribute the operator anomalous dimension.

where $\gamma_{\mathcal{O}}$ is the anomalous dimension. Calculating the Feynman diagrams in Fig. 6, we can obtain

$$\gamma_{\mathcal{O}} = -\frac{g_D^2}{24\pi^2} (1 - n_f), \quad (\text{A2})$$

where n_f is the number of fermion doublet as defined in Sec. III. A. The solution of the evolution equation (A1) is

$$C(\mu) = \exp \left[\int_{g_D(\Lambda)}^{g_D(\mu)} \frac{\gamma_{\mathcal{O}}(g_D)}{\beta(g_D)} dg_D \right] C(\Lambda). \quad (\text{A3})$$

Thus, the Wilson coefficient at M_Z scale becomes

$$C(M_Z) = \left(\frac{\alpha_D(M_Z)}{\alpha_D(m_1)} \right)^{1/20} \left(\frac{\alpha_D(m_2)}{\alpha_D(\Lambda)} \right)^{-1/16} C(\Lambda). \quad (\text{A4})$$

APPENDIX B: DECAY OF DARK GAUGE BOSONS AND DARK SCALARS

In this appendix, we discuss the decay properties of dark gauge bosons and dark Higgs bosons.

1. decay of \mathcal{Z}_1

The main decay channels of \mathcal{Z}_1 are $\mathcal{Z}_1 \rightarrow h_1 h_2$ and $\mathcal{Z}_1 \rightarrow h_1 \tilde{h}_3$. The total decay width is given by

$$\Gamma_{\mathcal{Z}_1} = \frac{\alpha_D M_{\mathcal{Z}}}{6\sqrt{2}} \left(1 - \frac{2M_{\mathcal{H}}^2}{M_{\mathcal{Z}}^2}\right) \sqrt{1 - \frac{2M_{\mathcal{H}}^2}{M_{\mathcal{Z}}^2}}. \quad (\text{B1})$$

For $M_{\mathcal{Z}} = 0.1\text{GeV}$, $M_{\mathcal{H}} = 0.02\text{GeV}$ and $\alpha_D(M_{\mathcal{Z}}) = 0.57$, we have $\Gamma_{\mathcal{Z}_1} \sim 0.006\text{GeV}$.

2. decay of \mathcal{Z}_2

The main decay channels of \mathcal{Z}_2 are $\mathcal{Z}_2 \rightarrow \gamma h_2$ and $\mathcal{Z}_2 \rightarrow f \bar{f}$ ($f = e^-, \nu_e, \nu_\mu, \nu_\tau$). For γh_2 channel, the decay width is

$$\Gamma_{\mathcal{Z}_2 \rightarrow \gamma h_2} = \frac{\alpha_D \epsilon^2 c_W^2 M_{\mathcal{Z}}}{12} \left(1 - \frac{M_{\mathcal{H}}^2}{M_{\mathcal{Z}}^2}\right)^3. \quad (\text{B2})$$

The decay width of channel $\mathcal{Z}_2 \rightarrow e^+ e^-$ is

$$\Gamma_{\mathcal{Z}_2 \rightarrow e^+ e^-} = \frac{\alpha \epsilon^2 c_W^2 M_{\mathcal{Z}}}{3} \left(1 + \frac{5m_e^2}{2M_{\mathcal{Z}}^2} - \frac{m_e^4}{2M_{\mathcal{Z}}^4}\right) \sqrt{1 - \frac{4m_e^2}{M_{\mathcal{Z}}^2}}, \quad (\text{B3})$$

where α is the fine structure constant. The decay widths $\Gamma_{\mathcal{Z}_2 \rightarrow \nu_i \bar{\nu}_i}$, ($i = e, \mu, \tau$) are negligible small. So the total decay width of \mathcal{Z}_2 can be written as

$$\Gamma_{\mathcal{Z}_2} = \frac{\alpha \epsilon^2 c_W^2 M_{\mathcal{Z}}}{3} \left(1 + \frac{5m_e^2}{2M_{\mathcal{Z}}^2} - \frac{m_e^4}{2M_{\mathcal{Z}}^4}\right) \sqrt{1 - \frac{4m_e^2}{M_{\mathcal{Z}}^2}} + \frac{\alpha_D \epsilon^2 c_W^2 M_{\mathcal{Z}}}{12} \left(1 - \frac{M_{\mathcal{H}}^2}{M_{\mathcal{Z}}^2}\right)^3. \quad (\text{B4})$$

For $M_{\mathcal{Z}} = 0.1\text{GeV}$, $M_{\mathcal{H}} = 0.02\text{GeV}$, $\epsilon = 10^{-5}$ and $\alpha_D(M_{\mathcal{Z}}) = 0.57$, we have $\Gamma_{\mathcal{Z}_2} \sim 3 \times 10^{-13}\text{GeV}$.

3. decay of \mathcal{Z}_3

The main decay channels of \mathcal{Z}_3 is $\mathcal{Z}_3 \rightarrow \gamma \tilde{h}_3$. The total decay width is

$$\Gamma_{\mathcal{Z}_3} = \frac{\alpha_D \epsilon^2 c_W^2 M_{\mathcal{Z}}}{24} \left(1 - \frac{M_{\mathcal{H}}^2}{M_{\mathcal{Z}}^2}\right)^3. \quad (\text{B5})$$

For $M_{\mathcal{Z}} = 0.1\text{GeV}$, $M_{\mathcal{H}} = 0.02\text{GeV}$, and $\alpha_D(M_{\mathcal{Z}}) = 0.57$, we have $\Gamma_{\mathcal{Z}_3} \sim 1.6 \times 10^{-13}\text{GeV}$.

4. decay of h_1

The main decay channels of h_1 are $h_1 \rightarrow f\bar{f}f'\bar{f}'$ where $f, f' = e^-, \nu_e, \nu_\mu, \nu_\tau$. For $M_Z = 0.1\text{GeV}$, $M_{\mathcal{H}} = 0.02\text{GeV}$ and $\alpha_D(M_Z) = 0.57$, the numerical result of the decay width shows that it is of order $O(10^{-35}\text{GeV})$.

5. decay of h_2

The dominant decay channels of h_2 are $h_2 \rightarrow \gamma f\bar{f}$ ($f = e^-, \nu_e, \nu_\mu, \nu_\tau$). The numerical calculation shows that $\Gamma_{h_2 \rightarrow \gamma \nu_i \bar{\nu}_i}$, ($i = e, \mu, \tau$) are negligible small. Neglecting the electron mass and the contribution from diagrams with the Z^0 boson in the internal line, the total decay width can be written as

$$\Gamma_{h_2} = \frac{\alpha \alpha_D c_W^4 \epsilon^4 M_{\mathcal{H}}}{72\pi} \left[-17 \frac{M_{\mathcal{H}}^2}{M_Z^2} + 42 - 24 \frac{M_Z^2}{M_{\mathcal{H}}^2} + 6 \left(1 - \frac{4M_Z^2}{M_{\mathcal{H}}^2} \right) \left(1 - \frac{M_Z^2}{M_{\mathcal{H}}^2} \right)^2 \ln \left(1 - \frac{M_{\mathcal{H}}^2}{M_Z^2} \right) \right]. \quad (\text{B6})$$

For $M_Z = 0.1\text{GeV}$, $M_{\mathcal{H}} = 0.02\text{GeV}$, $\epsilon = 10^{-5}$ and $\alpha_D(M_Z) = 0.57$, $\Gamma_{h_2} \sim 4 \times 10^{-32}\text{GeV}$.

6. decay of \tilde{h}_3

\tilde{h}_3 decays into e^+e^- . The decay width is

$$\Gamma_{\tilde{h}_3} = \frac{\epsilon_{\mathcal{H}}^2 M_{\mathcal{H}}}{32\pi^2 \alpha_D} \frac{m_e^2 M_Z^2}{m_H^4} \left(1 - \frac{4m_e^2}{M_{\mathcal{H}}^2} \right) \sqrt{1 - \frac{2m_e^2}{M_{\mathcal{H}}^2}}. \quad (\text{B7})$$

For $m_H = 115\text{GeV}$, $M_Z = 0.1\text{GeV}$, $M_{\mathcal{H}} = 0.02\text{GeV}$, $\epsilon_{\mathcal{H}} = 10^{-7}$ and $\alpha_D(M_Z) = 0.57$, the decay width of \tilde{h}_3 is $1.7 \times 10^{-35}\text{GeV}$.

-
- [1] J. Dunkley et al. (WMAP), *Astrophys. J. Suppl.* **180**, 306 (2009), 0803.0586.
 - [2] A. W. Strong et al., *Astron. Astrophys.* **444**, 495 (2005), astro-ph/0509290.
 - [3] J. Chang et al., *Nature* **456**, 362 (2008).
 - [4] O. Adriani et al. (PAMELA), *Nature* **458**, 607 (2009), 0810.4995.
 - [5] O. Adriani et al., *Phys. Rev. Lett.* **102**, 051101 (2009), 0810.4994.
 - [6] A. A. Abdo et al. (The Fermi LAT), *Phys. Rev. Lett.* **102**, 181101 (2009), 0905.0025.

- [7] D. P. Finkbeiner and N. Weiner, Phys. Rev. **D76**, 083519 (2007), astro-ph/0702587.
- [8] L. Bergstrom, T. Bringmann, and J. Edsjo, Phys. Rev. **D78**, 103520 (2008), 0808.3725.
- [9] M. Cirelli and A. Strumia (2008), 0808.3867.
- [10] V. Barger, W. Y. Keung, D. Marfatia, and G. Shaughnessy, Phys. Lett. **B672**, 141 (2009), 0809.0162.
- [11] J.-H. Huh, J. E. Kim, and B. Kyae, Phys. Rev. **D79**, 063529 (2009), 0809.2601.
- [12] N. Arkani-Hamed, D. P. Finkbeiner, T. R. Slatyer, and N. Weiner, Phys. Rev. **D79**, 015014 (2009), 0810.0713.
- [13] P.-f. Yin et al., Phys. Rev. **D79**, 023512 (2009), 0811.0176.
- [14] K. Ishiwata, S. Matsumoto, and T. Moroi, Phys. Lett. **B675**, 446 (2009), 0811.0250.
- [15] A. Ibarra and D. Tran, JCAP **0902**, 021 (2009), 0811.1555.
- [16] D. Hooper, A. Stebbins, and K. M. Zurek, Phys. Rev. **D79**, 103513 (2009), 0812.3202.
- [17] Q.-H. Cao, E. Ma, and G. Shaughnessy, Phys. Lett. **B673**, 152 (2009), 0901.1334.
- [18] P. Meade, M. Papucci, and T. Volansky (2009), 0901.2925.
- [19] D. Hooper and K. M. Zurek, Phys. Rev. **D79**, 103529 (2009), 0902.0593.
- [20] C. Cheung, J. T. Ruderman, L.-T. Wang, and I. Yavin, Phys. Rev. **D80**, 035008 (2009), 0902.3246.
- [21] K. Cheung, P.-Y. Tseng, and T.-C. Yuan, Phys. Lett. **B678**, 293 (2009), 0902.4035.
- [22] X.-J. Bi, X.-G. He, and Q. Yuan, Phys. Lett. **B678**, 168 (2009), 0903.0122.
- [23] S.-L. Chen, R. N. Mohapatra, S. Nussinov, and Y. Zhang, Phys. Lett. **B677**, 311 (2009), 0903.2562.
- [24] K. Ishiwata, S. Matsumoto, and T. Moroi (2009), 0903.3125.
- [25] A. A. El-Zant, S. Khalil, and H. Okada (2009), 0903.5083.
- [26] V. Barger, Y. Gao, W. Y. Keung, D. Marfatia, and G. Shaughnessy, Phys. Lett. **B678**, 283 (2009), 0904.2001.
- [27] P. Meade, M. Papucci, A. Strumia, and T. Volansky (2009), 0905.0480.
- [28] X.-G. He (2009), 0908.2908, and references therein.
- [29] R. Bernabei et al. (DAMA), Eur. Phys. J. **C56**, 333 (2008), 0804.2741.
- [30] D. Tucker-Smith and N. Weiner, Phys. Rev. **D64**, 043502 (2001), hep-ph/0101138.
- [31] F. Chen, J. M. Cline, and A. R. Frey, Phys. Rev. **D79**, 063530 (2009), 0901.4327.
- [32] F. Chen, J. M. Cline, and A. R. Frey (2009), 0907.4746.

- [33] E. Ma, *Annales Fond. Broglie* **31**, 285 (2006), hep-ph/0607142.
- [34] T. Hur, H.-S. Lee, and S. Nasri, *Phys. Rev.* **D77**, 015008 (2008), 0710.2653.
- [35] Q.-H. Cao, E. Ma, J. Wudka, and C. P. Yuan (2007), 0711.3881.
- [36] H. Sung Cheon, S. K. Kang, and C. S. Kim (2008), 0807.0981.
- [37] M. Fairbairn and J. Zupan, *JCAP* **0907**, 001 (2009), 0810.4147.
- [38] S. Profumo, K. Sigurdson, and L. Ubaldi (2009), 0907.4374.
- [39] M. Baumgart, C. Cheung, J. T. Ruderman, L.-T. Wang, and I. Yavin, *JHEP* **04**, 014 (2009), 0901.0283.
- [40] D. P. Finkbeiner, N. Padmanabhan, and N. Weiner, *Phys. Rev.* **D78**, 063530 (2008), 0805.3531.
- [41] E. Kolb and M. Turner, Addison-Wesley P.C. (1990).
- [42] K. Griest and D. Seckel, *Phys. Rev.* **D43**, 3191 (1991).
- [43] D. J. Gross and F. Wilczek, *Phys. Rev.* **D8**, 3633 (1973).
- [44] E. Churazov, R. Sunyaev, S. Sazonov, M. Revnivtsev, and D. Varshalovich, *Mon. Not. Roy. Astron. Soc.* **357**, 1377 (2005), astro-ph/0411351.
- [45] E. A. Baltz and J. Edsjo, *Phys. Rev.* **D59**, 023511 (1998), astro-ph/9808243.
- [46] M. Cirelli, R. Franceschini, and A. Strumia, *Nucl. Phys.* **B800**, 204 (2008), 0802.3378, and references therein.
- [47] R. Iengo (2009), 0903.0317.
- [48] G. J. Alner et al., *Astropart. Phys.* **28**, 287 (2007), astro-ph/0701858.
- [49] J. Angle et al. (XENON), *Phys. Rev. Lett.* **100**, 021303 (2008), 0706.0039.
- [50] Z. Ahmed et al. (CDMS), *Phys. Rev. Lett.* **102**, 011301 (2009), 0802.3530.
- [51] M. E. Peskin and T. Takeuchi, *Phys. Rev.* **D46**, 381 (1992).
- [52] K. S. Babu, C. F. Kolda, and J. March-Russell, *Phys. Rev.* **D57**, 6788 (1998), hep-ph/9710441.
- [53] I. Bars and M. Yoshimura, *Phys. Rev.* **D6**, 374 (1972).
- [54] C. Amsler et al. (Particle Data Group), *Phys. Lett.* **B667**, 1 (2008).
- [55] D. Stump et al., *Phys. Rev.* **D65**, 014012 (2001), hep-ph/0101051.
- [56] C. S. Li, Z. Li, and C. P. Yuan, *JHEP* **06**, 033 (2009), 0903.1798.
- [57] J. F. Navarro, C. S. Frenk, and S. D. M. White, *Astrophys. J.* **462**, 563 (1996), astro-ph/9508025.
- [58] M. Aguilar et al. (AMS-01), *Phys. Lett.* **B646**, 145 (2007), astro-ph/0703154.

- [59] R. L. Golden et al. (WIZARDS), *Astrophys. J.* **457**, L103 (1996).
- [60] M. Boezio et al., *Astrophys. J.* **532**, 653 (2000).
- [61] S. W. Barwick et al. (HEAT), *Astrophys. J.* **482**, L191 (1997), astro-ph/9703192.
- [62] K. K. Tang, *Astrophys. J.* **278**, 881 (1984).
- [63] M. A. DuVernois et al., *Astrophys. J.* **559**, 296 (2001).
- [64] S. Torii et al., *Astrophys. J.* **559**, 973 (2001).
- [65] F. Aharonian et al. (H.E.S.S.), *Phys. Rev. Lett.* **101**, 261104 (2008), 0811.3894.
- [66] N. Arkani-Hamed and N. Weiner, *JHEP* **12**, 104 (2008), 0810.0714.
- [67] A. Pukhov (2004), hep-ph/0412191.
- [68] E. Braaten, C.-S. Li, and T.-C. Yuan, *Phys. Rev. Lett.* **64**, 1709 (1990).